THE STRUCTURE OF THE HUMAN SUBCHONDRAL PLATE

J. M. CLARK, J. D. HUBER

From the University of Washington, Seattle

To study the anatomy of subarticular bone and cartilage, fresh specimens of cartilage on bone from the human shoulder, hip and knee were treated with bleach or papain, or were fixed and decalcified. All were compared using scanning electron microscopy. Papain digestion selectively removed cartilage to the tidemark. The tidemark contour was highly variable; irregularities were indirectly related to degenerative lesions and were most prominent in peripheral non-weight-bearing areas of joints with central fibrillation. Decalcification exposed the interface between the bone and calcified cartilage. Collagen fibrils in articular cartilage did not interdigitate with those of bone. The subchondral bone was appositional, avascular, smooth and very thin in most areas of human joints. Perforations through subchondral bone or calcified cartilage were rare. Bleach maceration destroyed important details.

The base of mature articular cartilage is a composite of calcified cartilage resting on a sheet of bone. We have studied the remodelling process and response to injury of these subchondral layers using various forms of microscopy and concentrating on three features: the thickness of the subchondral layers, the extent of their vascularisation and the advancement of the tidemark. Scanning electron microscopy (SEM) has been employed before to provide a three-dimensional description of the perforations in the bone plate (Bullough and Jagannath 1983; Duncan et al 1987) and of the collagen fibres in the calcified cartilage (Hough et al 1974; Redler et al 1975). The interface between the soft and the hard tissues is difficult to scan successfully. We report on several SEM techniques, adapted to provide vertical sections and facing views of the various cartilage layers.

METHODS

Tibial plateaux, femoral condyles and humeral heads from 20 human subjects were used for this study. These specimens provided fresh cartilage and most were never frozen. The subjects ranged in age from 17 to 70 years. Approximately three-quarters of the joints exhibited moderate degenerative changes, including superficial fibrillation and osteophytes, but none had frank erosions into the cartilage. To correlate degenerative changes with the structure of the subchondral plate, the tibial plateaux were photographed while fresh.

Our purpose was to examine and compare the structures exposed by bleach maceration, by papain digestion and by decalcification. Five lateral tibial plateaux, five medial femoral condyles and four humeral heads were each trimmed with a bandsaw into five, 5 mm-wide strips of cartilage resting on bone (Fig. 1a). The strips from each joint surface were then treated separately following the sequences (A, B, C, D and E) outlined in Table I.

Five lateral femoral condyles were cut into four, 5 mm-wide strips. These strips were broken in half while immersed in liquid nitrogen, to produce clean vertical sections through the cartilage. One half of each strip was

Table I. Treatment sequences used for specimen preparation

A: Fixation*/dehydration and cryofracture
B: Bleach maceration†/fixation/dehydration and cryofracture‡ (V)
C: Papain digestion§/fixation/dehydration and cryofracture (V)
D: Fixation/decalcification/dehydration and cryofracture (V)
E: Fixation/decalcification/dehydration and cryofracture (H, V)

*fixation; immersion for 24 hours in 2% glutaraldehyde in acetate buffer or cacodylate buffer.
†bleach maceration; immersion in 5% sodium hypochlorite for 24 hours at 25°C.
‡cryofracture; immersion in liquid nitrogen after dehydration, then broken with a sharp chisel while frozen (V, vertically; H, horizontally).
§papain digestion; immersion in papain 400U/l in acetate buffer, pH 7.2, for 24 hours at 40°C.

J. M. Clark, MD, PhD, Assistant Professor
J. D. Huber, Research Technologist
Department of Orthopaedics, RK-10, University of Washington, School of Medicine, Seattle, Washington 98195, USA.

Correspondence should be sent to Dr J. M. Clark.

© 1990 British Editorial Society of Bone and Joint Surgery
0301-620X/90/5205 $2.00
J Bone Joint Surg [Br] 1990; 72-B:866–73.

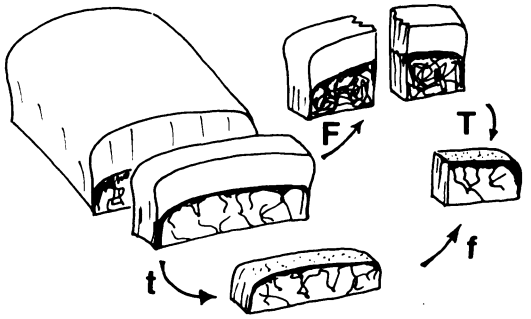

Fig. 1a

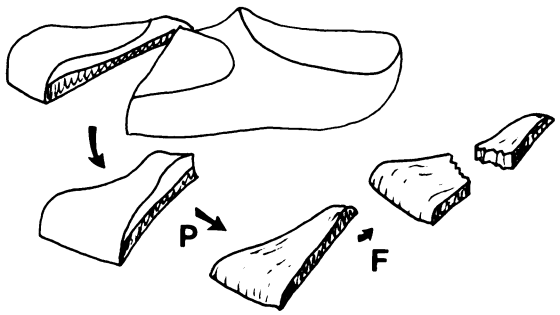

Fig. 1b

Figure 1a – Fresh cartilage on bone was cut into 5 mm-wide sequential slices. Each slice was freeze-fractured into halves (F). One half was fixed immediately; the other half was treated with papain, bleach or by decalcification (T). For the descriptive part of this study, the entire segment was treated while fresh (t), then dehydrated and fractured (f). These methods produced treated specimens from adjacent locations with vertical fractures and facing surfaces exposed for comparison. Figure 1b – Method used to expose the upper surface of calcified cartilage in the tibial plateau. The medial plateau was photographed and then cut into wedges which included peripheral and central joint surfaces. The specimen was treated with papain (P), fixed, dehydrated and cryofractured into halves or thirds (F).

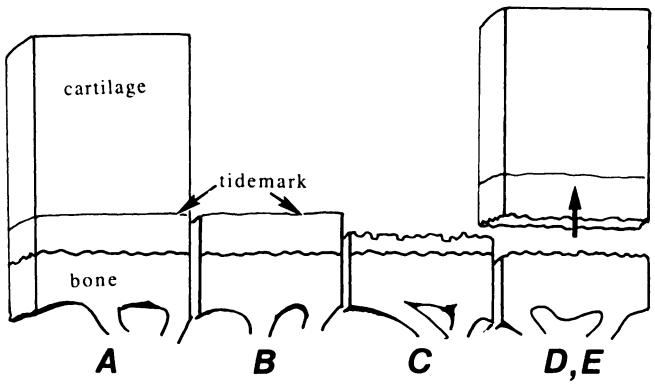

Fig. 2

Illustration of the effects of the different treatment sequences outlined in Table I: A) fixation alone; B) papain; C) bleach; D) decalcification and E) decalcification and cryofracture through the junction between bone and cartilage.

fixed immediately; the other half was treated following sequence B, C, D or E.

To study the morphology of the tidemark across a joint surface, wedges extending from the edge to the centre were cut from 12 medial tibial plateaux (Fig. 1b). These were all treated with papain (sequence C).

For comparison with the human material, specimens cut from tibial plateaux, femoral condyles and humeral heads of three mature rabbits, sacrificed by pentobarbitol injection, were treated with papain (sequence C) or decalcified (sequences D, E).

After treatment and fixation, each piece from each part of the study was examined under a binocular dissecting microscope at up to 60 × magnification. The colour, contour and any perforations in the surface were observed and recorded. The specimens were then washed and dehydrated in ethanol. To create clean sections for SEM, those not previously fractured were frozen in liquid nitrogen and 'cryofractured' vertically (Humphreys, Spurlock and Johnson 1974, 1975). One set of decalcified strips was fractured both vertically and transversely (group E). These transverse fractures were made parallel to the joint surface at the approximate level of the interface between bone and cartilage.

All specimens to be viewed by SEM were critical point-dried, mounted on Cambridge mounts (Pella Inc, Redding, California), gold-coated and viewed on a JEOL JSM 35c microscope. To confirm the level of calcification in the fractured specimens, the vertical surfaces were imaged in the back-scatter mode at 15 to 35 kV (Becker and Geoffroy 1981; Boyde and Jones 1983).

In this paper, the layers of cartilage are named according to the scheme used by Lane and Weiss (1975). The subchondral bone and calcified cartilage are together termed the 'subchondral plate' (Duncan et al 1987). A collagen 'fibril' is the smallest separate fibrillar unit visible by SEM, and a 'fibre' is any bundle of parallel fibrils. The term 'tidemark' denotes the border between calcified and uncalcified cartilage rather than the specific line seen on light micrographs.

RESULTS

The above methods yielded five specimens from each of the human joint surfaces (Fig. 2). In one (A), the cartilage was intact; in the other four it had been partially or completely removed and facing views of the remaining cartilage or bone were presented. Usually, one side of a specimen was cleanly fractured so that a vertical section through the subchondral plate was also exposed for SEM. For a subset of these treated preparations, an intact, untreated half of each specimen was available for direct comparison along a common fractured interface.

Fractured preparations. By SEM, the general appearance of the untreated (group A) articular cartilage was similar to that reported by others (Clark 1985). The level of the tidemark, defined here as the junction between calcified and uncalcified cartilage, was readily identified because the calcified cartilage was more dense and homogeneous (Figs 3 and 4). This is best seen with back-scatter imaging (Fig. 3a). No linear structure corresponding to the tidemark was seen on any of the SEM preparations. At magnifications of greater than 200 ×, distinction between subchondral bone and calcified cartilage was usually possible, because the lamellae in the bone were visible (Fig. 4).

calcified cartilage and subchondral bone. In preparations where the fracture lay parallel to the fibres, their constituent fibrils could be traced individually from the calcified zone into the uncalcified cartilage. The fibres appeared slightly more compact in the calcified layer than in the uncalcified, so that the level of the pre-existing tidemark could be identified. Collagen fibrils never crossed between the bone and the cartilage but ended abruptly, as if cut where they met bone (Fig. 6b).

The lamellae and osteocyte lacunae in the subchondral bone were clearly visible in all the fractured SEM preparations (Fig. 7). Cells were seen in those specimens not treated with papain or bleach. In the subchondral

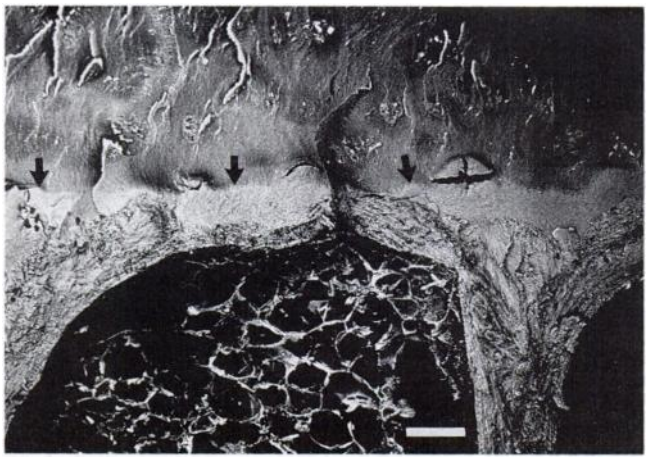

Fig. 3a

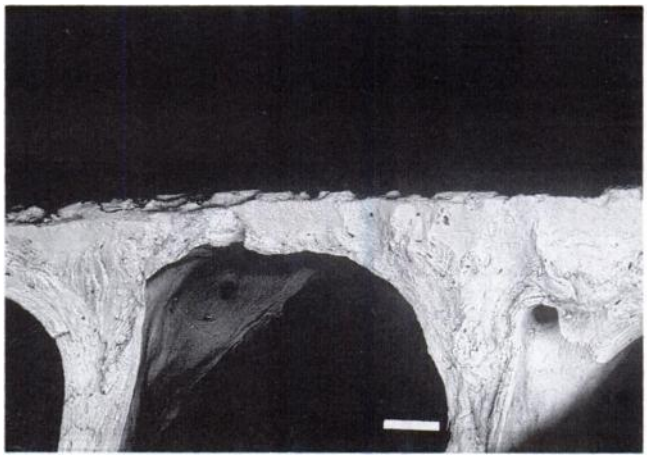

Fig. 3b

Human femoral condyle. Figure 3a – Specimen fixed immediately after freeze-fracture, viewed in the back-scatter mode of SEM. The calcified cartilage appears lighter than the adjacent uncalcified cartilage, permitting accurate localisation of the tidemark (arrows). Figure 3b – Specimen treated with papain. The surface shown here was broken away from that in 3a and shows its mirror image. Comparison of the two images shows that the cartilage was removed only to the level where it was calcified.

Papain (sequence C) and bleach (sequence B) both removed all the uncalcified articular cartilage after 24 hours of exposure (Fig. 3). Papain did not digest the collagen below the tidemark, but bleach often removed the calcified cartilage, either partially or completely (Figs 3 and 5). The thickness and contour of the calcified zone in papain-treated cartilage was similar to that of the untreated side, but after bleach treatment the calcified zone was thinned irregularly and, near the periphery, the subchondral bone was eroded. We therefore based our conclusions about the structure of the calcified zone upon the untreated and the papain-treated specimens (groups A and C).

Following decalcification (sequence D), the border between the bone and the cartilage was more clearly defined than in mineralised specimens (Fig. 6). Usually, a narrow gap was visible between the two layers and the decalcified cartilage could be peeled from the bone of the humeral head.

Decalcification also exposed the collagen fibrils in

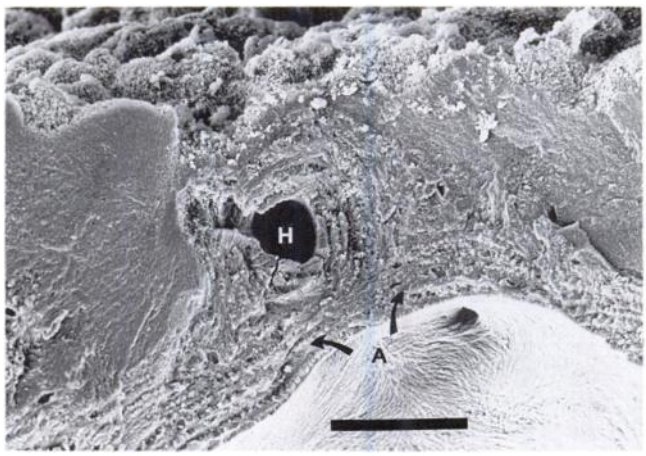

Fig. 4

Femoral condyle following papain treatment and fracture (sequence C). The bone is distinct from calcified cartilage because of its lamellar structure. The two forms of lamellae are shown here: concentric layers about a haversian canal (H) and appositional layers where the bone faces the marrow cavity (A). Mark = 100 μm.

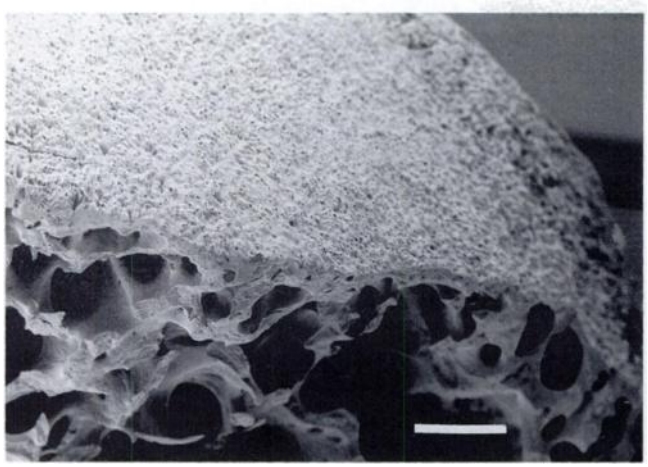

Fig. 5a

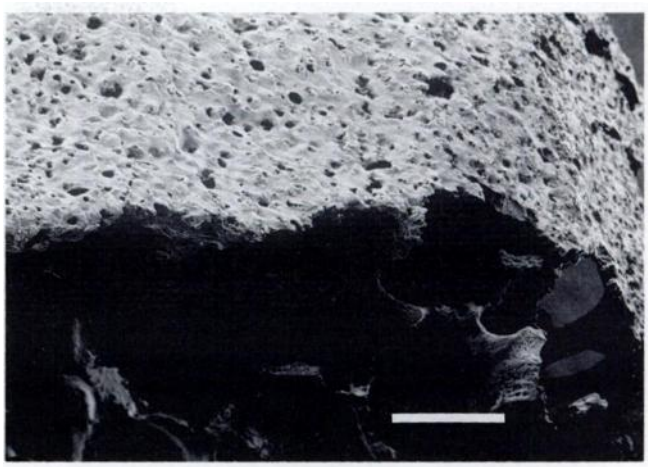

Fig. 5b

Femoral condyle. Comparison of papain (a) and bleach treatment (b). These adjacent specimens show that bleach eroded through the plate in many areas, creating perforations. Mark = 1000 μm.

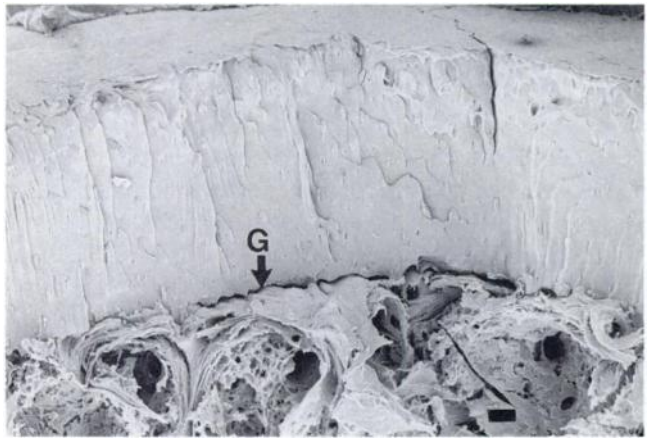

Fig. 6a

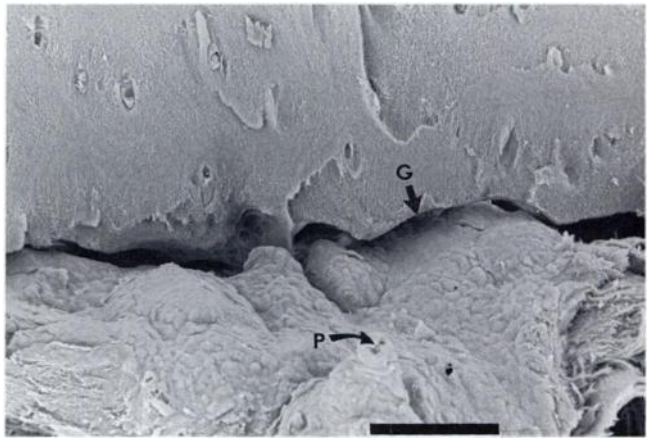

Fig. 6b

Fig. 6c

Figure 6. Humeral head, decalcified (sequence D). a) Following decalcification, a narrow gap (G) was present between cartilage and subchondral bone. The arched layers of subchondral bone are formed from multiple appositional layers. Mark = 100 μm; b) This detail shows the small mounds typical of subchondral bone in human joints. The bone was solid except for rare perforations as seen in the foreground (P). Mark = 100 μm; c) Thin appositional subchondral bone. The lamellae (arrows) can be traced through the bone after decalcification because the collagen fibres are exposed. Fat cells fill the marrow space at the right. Mark = 10 μm.

bone, lamellae of two types were present; some formed concentric layers about vascular canals typical of osteons (see Fig. 4), and others were flat and appeared to represent appositional layers formed under the endosteum (Figs 6a, 6c and 7). The deep surface of the subchondral bone was composed of multiple layers of appositional bone which extended down onto the supporting trabeculae and formed arches. Occasional conical areas were found where the lamellae had been replaced by separate systems typical of filled-in Howship's lacunae (Fig. 7).

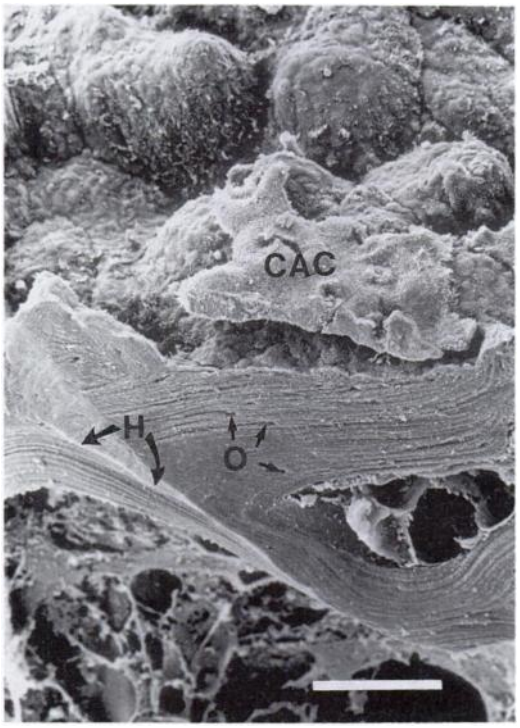

Fig. 7

Tibial plateau which has been decalcified and fractured horizontally as well as vertically (sequence E). The vertical surface shows osteocyte lacunae (O) and lamellae in the bone. Lamellae fill a Howship's lacuna (H). The horizontal fracture has removed all but a fragment of the cartilage (CAC) and the nodular surface of the bone is exposed. Mark = 100 μm.

Because the junction of cartilage and bone was visible at lower magnifications following decalcification, it was possible to define the thickness and composition of subchondral bone at different locations. The bone was thin (as little as 10 μm) in all locations studied except at the centre of the tibial plateau, where it was up to 3 mm thick (Figs 8 and 9). This thin bone was constructed mainly of appositional layers continuous with trabeculae; haversian canals were seldom seen. However, where the subchondral bone was exceptionally thick beneath the centre of degenerated tibial plateau, it was composed primarily of an irregular network of osteons (Fig. 9a).

***En face* preparations.** Several of the treatment sequences used produced facing views of layers in the subchondral plate (Fig. 2). Papain reliably removed the cartilage down to the tidemark (group C) (Figs 3, 4, 8 and 9). Decalcification alone or in combination with fracture separated the articular cartilage from bone (groups D and E) (Figs 6b and 7). As described above, the cartilage could be peeled from the humeral head following decalcification. Tangential fractures directed through the subchondral region of decalcified specimens also separated the cartilage from bone.

The superficial surface of the calcified cartilage exposed by papain digestion was uniformly covered with empty cell lacunae (Figs 8 and 9). Ridges and grooves in the calcified cartilage were associated with the presence of degenerative changes in the overlying articular cartilage. The tidemark was relatively smooth directly under areas of fibrillation, which were always in the centre of the specimens studied here (Fig. 8a). These areas of roughness occurred mainly on the tibial plateau in the areas covered by a meniscus (Figs 8b and 9b). No configuration which could be interpreted as 'duplication' of the tidemark was seen.

Actual perforations through the subchondral plate, that is through the calcified cartilage and the subchondral bone, were found only in the tibial plateau. They were rare (fewer than 10 /cm^2) and more common at the periphery where the subchondral bone was thin. Because of the marked irregularity often present in the upper surface of the calcified cartilage, deep folds were easily mistaken for perforations in low-power views. Vertical fractures through the papain-treated specimens, however, confirmed that these crevices seldom extended through the plate (Figs 8 and 9). No relationship between degenerative changes in the cartilage and perforations in the plate was observed.

The facing views of the bone produced by fracturing or stripping away the cartilage revealed a surface covered by uniform knob-like prominences (Fig. 6b). Small (20 μm) perforations were occasionally found at the apices of these bony prominences (Fig. 6b), and these perforations through the bone could also be identified on vertical fractures through the subchondral plate. Most of the prominences contained a narrow central channel.

DISCUSSION

We have examined the two principal fronts in the region of subarticular bone and cartilage: the tidemark, which represents the upper limit of calcification in articular cartilage, and the osteochondral junction. We found that the subchondral bone plate had relatively distinct borders. Collagen fibres of the cartilage do not penetrate into the bone, and pores which cross through it into calcified or uncalcified cartilage are rare. The differences between these findings and those reported by others can be explained by differences in technique.

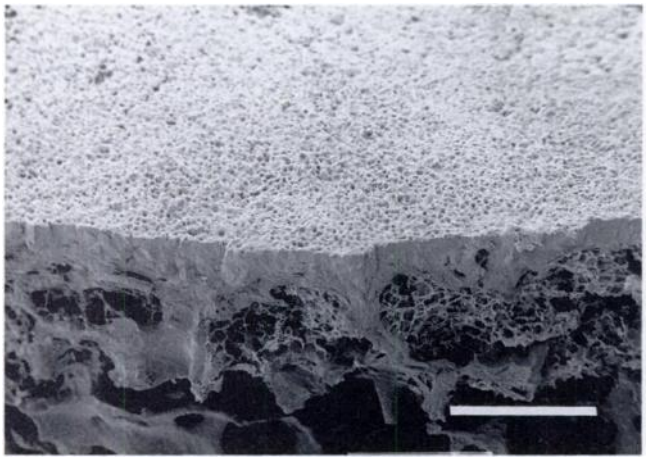

Fig. 8a

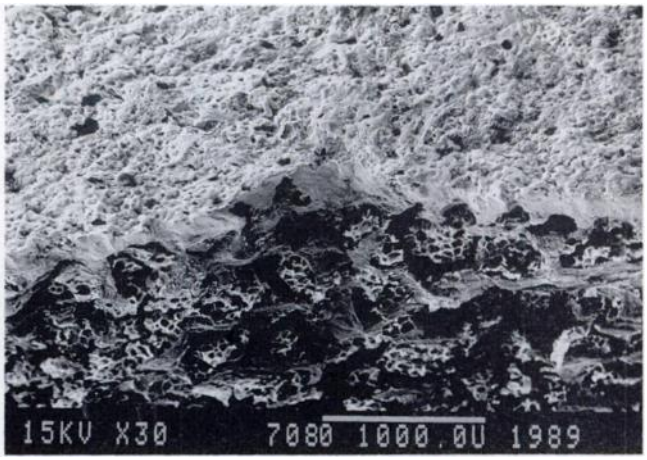

Fig. 8b

Figure 8. Tibial plateau, with minimal fibrillation of cartilage, after treatment with papain. a) In this specimen from the centre of the joint, the upper surface of the calcified cartilage is smooth and the plate is of modest thickness. Mark = 1000 μm; b) At the periphery of the same joint surface the tidemark is somewhat convoluted and the subchondral plate is thin. Mark = 1000 μm.

Figure 9. Tibial plateau, with moderate fibrillation of cartilage, after treatment with papain. a) In this specimen from the centre of the joint, the subchondral bone is thick, and laced with numerous haversian canals. The tidemark is smooth. Mark = 100 μm; b) At the periphery, the plate is thinner and the upper surface of the calcified cartilage is irregular. None of the involutions seen on the surface extended through the plate. Mark = 100 μm.

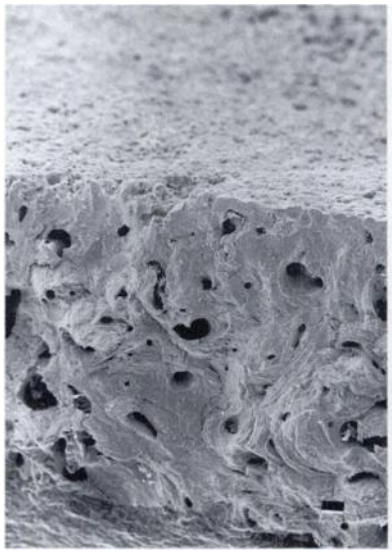

Fig. 9a

Fig. 9b

Previous SEM studies have often relied on 'anorganic' preparations which expose the subchondral plate through removal of the overlying uncalcified cartilage (Boyde and Hobdell 1969; Fujimoto et al 1980; Wampler, Tebo and Pinero 1980; Lester, Ash and Lillie 1981; Bullough and Jagannath 1983; Duncan et al 1987). Bleach maceration and other processes used to remove the organic matrix are perhaps too destructive. Bullough and Jagannath (1983) used both hydrazine and heat to produce anorganic preparations and noted that the thinner areas of the subchondral surface were sometimes damaged. Duncan et al (1987) ascribed cracks in their preparations to the maceration process. Without its supporting fibrous framework, the subchondral tissues are fragile and readily collapse. We observed that papain at neutral pH reliably preserved the structures of the calcified cartilage. Arsenault and Hunziker (1988) have shown that the mineral in calcified cartilage is bound to the collagen fibrils as it is in bone. The enzyme does not remove the collagen from these calcified tissues, probably because the calcium salt physically protects the fibril from the papain molecule.

Decalcification alone and in combination with freeze fracture is an effective means of exposing the interface between bone and cartilage for study by SEM. Frasca, Harper and Katz (1977) noted that decalcification delineated the lamellae in bone by exposing their collagen fibrils, and that manipulation of the specimens created planes in the tissue. Hough et al (1974), also using SEM on decalcified specimens, looked at sections which had been embedded, cut and etched by removal of the embedding medium. Our findings contradict their obser-

vation that the collagen fibres of bone and cartilage interdigitate. In our hands, removal of embedding resin causes tissue to coalesce into a mat and cannot be used for studying collagen fibril relationships.

Duncan et al (1987) reported the appearance of numerous holes perforating the calcified cartilage in bleach-macerated human tibial plateaux. They suggested that the holes could represent either vascularisation of the cartilage or collapse of the subchondral plate and incipient cyst formation. We found some holes in papain-treated plateaux, but our survey of 12 medial tibial plateaux indicated that perforations greater than 20 μm wide were quite rare. Penetration of the bone by a vessel was unusual.

The false SEM appearance of holes in the subchondral plate may be created in two ways. First, through the destructive action of chemical maceration; as explained, the thin areas in the human plate do not survive this process. Secondly, determination of the depth of a hole or crevice from facing micrographs is difficult. Vertical fractures through the same material revealed that most of the indentations in the calcified cartilage did not communicate with vascular canals or marrow spaces. Because of the limitations of all methods which produce facing views, their use should be combined with vertical sections of intact tissue, as Lane, Villacin and Bullough (1977) did in their study of shaved joint surfaces. They observed as many as 400 vessels per 64 mm^2 in the subchondral region of the femoral head when looking down onto the intact plate, but went on to show, by sectioning the tissue for light microscopy, that these vessels did not necessarily cross the tidemark.

The upper surface of the calcified zone exposed by papain treatment was very irregular in some subjects. This irregularity was greatest at the periphery of the tibial plateau, and was proportional to the amount of degenerative change present at the centre. At the centre of a moderately degenerative joint, the subchondral plate was very thick, indicating higher stresses, and the tidemark was relatively smooth. The studies of Harrison, Schajowicz and Trueta (1953), Haynes (1980), and Meachim and Allibone (1984) all showed that duplication and irregularity of the tidemark was more evident in the non-weight-bearing areas of the femoral head, and that advancement of calcification is more rapid there. Our findings suggest a similar phenomenon on the tibial plateau. This could represent a mechanism whereby low-pressure areas are brought into better contact with opposing surfaces, as suggested by Goodfellow and Bullough (1967).

The structure of the subchondral bone plate should shed light on the process by which it is formed. Meachim and Allibone (1984) found that subchondral bone is composed of two types of lamellae: concentric layers around osteons and flat layers typical of appositional new bone formation. However, we observed mature osteons only in the thickened plate beneath the central tibial plateau; this haversian bone resembled vascular cortex. The thin peripheral bone was virtually avascular, as are trabeculae, and the endosteal bone abutted directly on calcified cartilage. These findings suggest that, if the cartilage is replaced through vascular invasion and endochondral ossification, complete remodelling must subsequently occur.

Several studies have reported irregularity of the subchondral bone underlying injured degenerative cartilage (Wampler et al 1980). The facing views of bone produced here by decalcification and mechanical separation from the cartilage show that this irregularity takes the form of knob-like protuberances. From their shape and central canals, the larger knobs appear to be bone formed around vessels. Roughness of the bone may reflect a period of vascular invasion, since both irregularity and vascularity of the bone are associated with remodelling of the subchondral plate (Lemperg 1971; Lane et al 1977; Donohue et al 1983).

Because calcification of cartilage is closely associated with remodelling and may not always be confined to areas beneath the haematoxylin-stained tidemark (Green et al 1970; Lane and Bullough 1980; Meachim and Allibone 1984), an accurate marker of its distribution is useful. Back-scatter electron imaging with SEM is effective in this application. Unlike Redler et al (1975), we were unable to visualise the tidemark as a distinct linear structure using conventional SEM. The back-scatter mode, however, confirmed the exact upper margin of calcification so that, in any undecalcified specimen, we were confident of this landmark. We also used the back-scatter mode to confirm the effectiveness of decalcification and enzymatic removal of uncalcified cartilage.

Previous studies, as well as the work reported here, indicate that anatomy of the subchondral region is highly variable. These variations include the contour of the tidemark and cement line, the number and type of perforations in the plate and the thickness and composition of the subchondral bone. SEM is an effective tool for exploring these features if combined with techniques which expose broad facing surfaces.

This work was supported by a grant from the Orthopaedic Research and Education Foundation (No. 87-4-CO).

No benefits in any form have been received or will be received from a commercial party related directly or indirectly to the subject of this article.

REFERENCES

Arsenault AL, Hunziker EB. Electron microscopic analysis of mineral deposits in the calcifying epiphyseal growth plate. *Calcif Tissue Int* 1988; 42:119-26.

Becker RP, Geoffroy JS. Backscattered electron imaging for the life sciences – introduction and index to applications– 1961 to 1980. *SEM* 1981; IV:195-206.

Boyde A, Hobdell MH. Scanning electron microscopy of lamellar bone. *Z Zellforsch* 1969; 93:213-31.

Boyde A, Jones SJ. Back-scattered electron imaging of skeletal tissues. *Metab Bone Dis Relat Res* 1983; 5:145-50.

Bullough PG, Jagannath A. The morphology of the calcification front in articular cartilage: its significance in joint function. *J Bone Joint Surg [Br]* 1983; 65-B:72-8.

Clark JM. The organization of collagen in cryofractured rabbit articular cartilage: a scanning electron microscopic study. *J Orthop Res* 1985; 3:17-29.

Donohue JM, Buss D, Oegema TR Jr, Thompson RC. The effects of indirect blunt trauma on adult canine articular cartilage. *J Bone Joint Surg [Am]* 1983; 65-A:948-57.

Duncan H, Jundt J, Riddle JM, Pitchford W, Christopherson T. The tibial subchondral plate. *J Bone Joint Surg [Am]* 1987; 69-A: 1212-20.

Frasca P, Harper RA, Katz JL. Collagen fiber orientations in human secondary osteons. *Acta Anat* 1977; 98:1-13.

Fujimoto M, Egawa K, Ide Y, Takiguchi R. Scanning electron microscopy of calcifying cartilage matrix in the mandibular condyle. *Bull Tokyo Dent Coll* 1980; 21(1):41-7.

Goodfellow JW, Bullough PG. The pattern of ageing of the articular cartilage of the elbow joint. *J Bone Joint Surg [Br]* 1967; 49-B: 175-81.

Green WT, Martin GN, Eanes ED, Sokoloff L. Microradiographic study of the calcified layer of articular cartilage. *Arch Path* 1970; 90: 151-8.

Harrison MHM, Schajowicz F, Trueta J. Osteoarthritis of the hip: a study of the nature and evolution of the hip disease. *J Bone Joint Surg [Br]* 1953; 35-B:598-626.

Haynes DW. The mineralization front of articular cartilage. *Metab Bone Dis Relat Res* 1980; 2-S:55-9.

Hough AJ, Banfield WG, Mottram FC, Sokoloff L. The osteochondral junction of mammalian joints. *Lab Invest* 1974; 31(6):685-95.

Humphreys WJ, Spurlock BO, Johnson JS. Critical point drying of ethanol-infiltrated, cryofractured biological specimens for scanning electron microscopy. *SEM* 1974; Pt I:275-82.

Humphreys WJ, Spurlock BO, Johnson JS. Transmission electron microscopy of tissue prepared for scanning electron microscopy by ethanol-cryofracturing. *Stain Technol* 1975; 50(2):119-25.

Lane JM, Weiss C. Review of articular cartilage collagen research. *Arthritis Rheum* 1975; 18:553-62.

Lane LB, Villacin A, Bullough PG. The vascularity and remodelling of subchondral bone and calcified cartilage in adult human femoral and humeral heads: an age- and stress-related phenomenon. *J Bone Joint Surg [Br]* 1977; 59-B:272-8.

Lane LB, Bullough PG. Age-related changes in the thickness of the calcified zone and the number of tidemarks in adult human articular cartilage. *J Bone Joint Surg [Br]* 1980; 62-B:372-5.

Lemperg R. The subchondral bone plate of the femoral head in adult rabbits. II. Changes induced by intracartilaginous defects studied by microradiography and tetracycline labelling. *Virchows Arch A (Pathol Anat)* 1971; 352:14-25.

Lester KS, Ash MM, Lillie JH. Condylar cartilage: a scanning electron microscope study of anorganic mammalian condyles. *J Prosthet Dent* 1981; 45:422-9.

Meachim G, Allibone R. Topographical variation in the calcified zone of upper femoral articular cartilage. *J Anat* 1984; 139(2):341-52.

Redler I, Mow VC, Zimny ML, Mansell J. The ultrastructure and biomechanical significance of the tidemark of articular cartilage. *Clin Orthop* 1975; 112:357-62.

Wampler HW, Tebo HG, Pinero GJ. Scanning electron microscopic and radiographic correlation of articular surface and supporting bone of the mandibular condyle. *J Dent Res* 1980; 59(5): 754-61.